Laser-Induced Fluorescence Spectra of 4-Methylcyclohexoxy Radical and Perdeuterated Cyclohexoxy Radical and Direct Kinetic Studies of Their Reactions with O_2

Lei Zhang,[†] Karen M. Callahan,[‡] Dean Derbyshire,[§] and Theodore S. Dibble*[,†]

Department of Chemistry, SUNY - Environmental Science and Forestry, 1 Forestry Drive, Syracuse, New York 13210, Department of Biochemistry, The Ohio State University, Columbus, Ohio 43210, and Department of Chemistry, Le Moyne College, Syracuse, New York 13214

Received: March 29, 2005; In Final Form: August 17, 2005

The laser-induced fluorescence (LIF) excitation spectra of the 4-methylcyclohexoxy and d11-cyclohexoxy radicals have been measured for the first time. LIF intensity was used as a probe in direct kinetic studies of the reaction of O_2 with *trans*-4-methylcyclohexoxy and d11-cyclohexoxy radicals from 228 to 301 K. Measured rate constants near room temperature are uniformly higher than the Arrhenius fit to the lower-temperature data, which can be explained by the regeneration of cyclic alkoxy radicals from the product of their β-scission and the effect of O_2 concentration on the extent of regeneration. The Arrhenius expressions obtained over more limited ranges were $k_{O_2} = (1.4^{+8}_{-1}) \times 10^{-13}$ exp[$(-810 \pm 400)/T$] cm^3 molecule^{-1} s^{-1} for *trans*-4-methylcyclohexoxy (228−292 K) and $k_{O_2} = (3.7^{+4}_{-1}) \times 10^{-14}$ exp)[(-760 ± 400) /T] cm^3 molecule^{-1} s^{-1} for d11-cyclohexoxy (228−267 K) independent of pressure in the range 50−90 Torr. The room-temperature rate constant for the reaction of *trans*-4-methylcyclohexoxy radical with O_2 (obtained from the Arrhenius fit) is consistent with the commonly recommended value, but the observed activation energy is ∼3 times larger than the recommended value of 0.4 kcal/mol and half the value previously found for the reaction of normal cyclohexoxy radical with O_2.

Introduction

The degradation of VOCs in polluted air produces alkoxy radicals via reaction of peroxy radicals with NO. The atmospheric fate of large alkoxy radicals ($\geq C_4$) is usually determined by competition among β C−C scission, reaction with O_2, and isomerization,[1−3] as shown for cyclohexoxy radical in Scheme 1. Different reaction pathways of the alkoxy radicals contribute differently to the formation of ozone and secondary organic aerosols;[4] therefore, understanding alkoxy radical chemistry in the atmosphere is of crucial importance for understanding and modeling smog chemistry.

Vehicle exhaust and evaporation of gasoline are important sources for the emission of cycloalkanes and substituted cycloalkanes in urban areas.[5] To date, the kinetics of small acyclic alkoxy radicals has received much attention, and several smog chamber studies have focused on cyclohexoxy radicals,[6−9] but no kinetic information has been reported on any of the isomers of the methylcyclohexoxy radical. The six-member ring of cyclohexoxy radicals is also a feature of alkoxy radicals from terpenes, which are very important in atmospheric chemistry due to their large emissions and their role in aerosol formation.[10] Kinetic studies of alkoxy radicals formed from cyclohexane and methylcyclohexane may provide insights into alkoxy radicals derived from terpenes, for which there are no *direct* experimental studies. Also, because we previously found an unexpectedly high activation energy for the reaction of cyclohexoxy with O_2,[11] it is interesting to investigate the kinetics of related radicals reacting with O_2.

SCHEME 1 : Potential Reaction Pathways of the Cyclohexoxy Radical

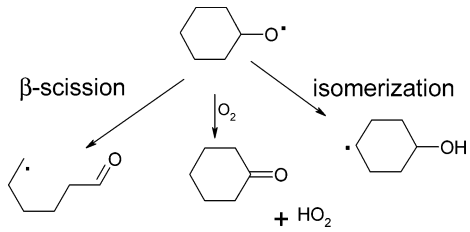

Considerations of the low Arrhenius preexponential (A) factor for RO• + O_2 reactions had led to considerable debate about the mechanism of this reaction. The concept of an ROOO• intermediate received some support from quantum calculations on CH_3O• + O_2,[12] but higher-level calculations by Bofill et al., strongly suggest that the CH_3OOO• species does not lead to reaction.[13] Instead, their results indicate that the *A* factor for abstraction is low due to noncovalent interactions between the radical center and the O atom of molecular oxygen that is *not* abstracting the hydrogen atom. Building on this work, Setokuchi et al., have investigated dynamical effects on the rate constant for RO• + O_2 reactions, where R = CH_3, C_2H_5, and C_3H_7.[14] Nevertheless, our understanding of RO• + O_2 reactions is far from complete, even for these simple examples, and more computational and experimental work is needed.

The technique of laser-induced fluorescence (LIF) has long been used to monitor small alkoxy radicals (C_1−C_3) in direct kinetic studies due to its excellent sensitivity, selectivity, and time resolution.[15−24] More recently, spectroscopic and kinetic

* To whom correspondence should be addressed. Fax: (315) 470-6856. E-mail: tsdibble@syr.edu.
[†] SUNY - Environmental Science and Forestry.
[‡] The Ohio State University.
[§] Le Moyne College.

10.1021/jp051595t CCC: $30.25
Published on Web 00/00/0000 PAGE EST: 8.9

investigations have been extended to larger alkoxy radicals,[25−30] including cyclohexoxy radical.[11] Spectroscopic investigations of many of these larger alkoxy radicals have also been carried out under jet-cooled conditions.[31−35] Due, in large part, to the lack of any LIF spectra for substituted cyclohexoxy radicals, there have been no previous direct studies of their reaction kinetics.

The rest of this paper is organized as follows: the experimental and computational methods are discussed immediately below. We then present LIF excitation spectra of the 4-methylcyclohexoxy and d11-cyclohexoxy radicals, their spectroscopic analyses, and their conformational assignments. The discussion then turns to the temperature and pressure dependence of the absolute rate constant, k_{O_2}, for the reaction of the *trans*-4-methylcyclohexoxy and d11-cyclohexoxy radicals with O_2. Next, comparisons are made to the O_2 reaction rates of other alkoxy radicals, and we examine a number of factors that could confound the analysis of our kinetic data. Finally, we present a model of how β-scission influences the measured rate constants for the O_2 reactions of cyclic alkoxy radicals.

Experimental and Theoretical Methods

The method and apparatus used here are more fully described in refs 11 and 28; only a summary will be given here. An excimer laser (GAM Laser, Inc., EX100H) operating at 351 nm was used to photolyze vapor of 4-methylcyclohexyl nitrite or d11-cyclohexyl nitrite to generate the corresponding 4-methylcyclohexoxy or d11-cyclohexoxy radicals. A dye laser (Lambda Physik, FL3002) pumped by another excimer laser (Lambda Physik, Lextra 100, 308 nm) was used to excite the radicals. The fluorescence signal from the radicals was converted into electric signal by a photomultiplier tube, analyzed by a boxcar recorder, and transferred to a computer.

The excitation (probe) laser was scanned over the region from 346 to 377 nm, with a 5 μs delay time between the photolysis laser and excitation laser (at 227 K and 50 Torr N_2). In our studies, we observed a significant fluorescence signal when the photolysis laser was blocked. Therefore, in obtaining spectra of the radicals, we subtracted a background obtained with nitrite in the chamber but with the photolysis laser blocked. We verified that the overall signal strengths decreased significantly when the delay times between the photolysis and excitation lasers were extended from 5 μs to 10 ms.

In the kinetic experiments, the dye laser was fixed at one of three different excitation wavelengths: 354.246, 351.160, and 349.910 nm for the 4-methylcyclohexoxy radical and 347.446, 365.731, and 352.802 nm for the d11-cyclohexoxy radical. These wavelengths are marked by stars in Figures 1 and 2.

The nitrites were synthesized by the dropwise addition of a mixture of sulfuric acid and the corresponding alcohol to an aqueous sodium nitrite solution[36] and purified by trap-to-trap distillation. The well-established mechanism of nitrite synthesis is shown in Scheme 2.[37] Because the C−O bond of the alcohol is not broken, the configuration (cis or trans) of 4-methylcyclohexyl nitrite is expected to retain that of the starting alcohol. FTIR[38] and NMR[38] spectra were obtained to verify the structure and purity of all the nitrites. In this research, 4-methylcyclohexyl nitrites were synthesized as isomerically pure forms and as mixtures of trans and cis isomers from the corresponding alcohols: pure *trans*-4-methylcyclohexanol (97%, Aldrich Inc.), pure *cis*-4-methylcyclohexanol (98%, Acros Inc.), and a mixture of *trans*- and *cis*-4-methylcyclohexanol (99%, Aldrich Inc.). The purity of the 4-methylcyclohexyl nitrites was confirmed by GC/MS (Hewlett-Packard GC: 5890 Series II and MS: 5898A). GC analysis of 4-methylcyclohexyl nitrite confirmed the starting alcohols were the only major impurities in the nitrites: *cis*-4-

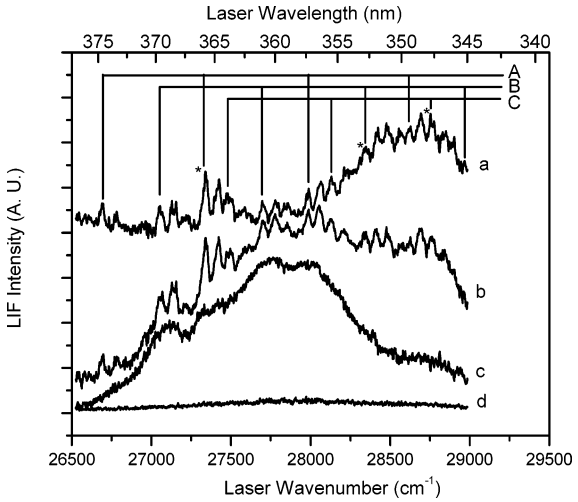

Figure 1. Laser-induced fluorescence (LIF) excitation spectrum of the d11-cyclohexoxy radical at 227 K and 50 Torr N_2. The partial pressure of d11-cyclohexyl nitrite was 6.5 mTorr. Peaks used in the kinetics experiments are marked with a *. Spectra: (a) spectrum of d11-cyclohexoxy; (b) overall spectrum of d11-cyclohexoxy and d11-cycloheoxyl nitrite; (c) spectrum of d11-cyclohexyl nitrite; (d) background of instrument (spectrum without d11-cyclohexyl nitrite). Spectra have been displaced vertically for ease of comparison.

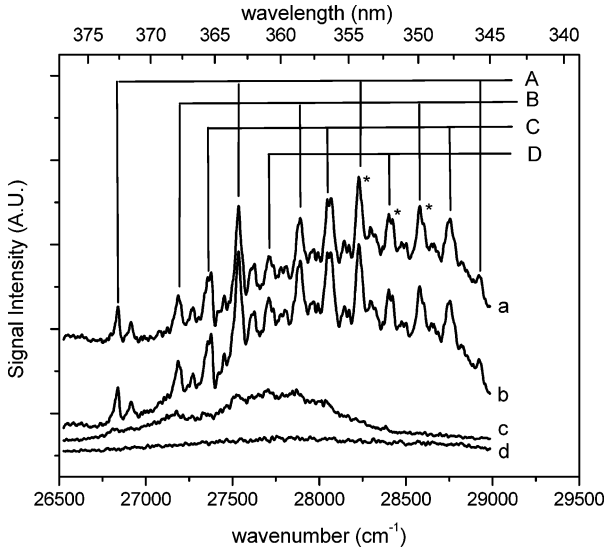

Figure 2. Laser-induced fluorescence (LIF) excitation spectrum of the 4-methylcyclohexoxy radical at 227 K and 50 Torr N_2. The partial pressure of the mixture of *cis*- and *trans*-4-methylcyclohexyl nitrite was 6.5 mTorr. Peaks used in the kinetics experiments are marked with a *. Spectra: (a) spectrum of 4-methylcyclohexoxy; (b) overall spectrum of 4-methylcyclohexoxy and 4-methylcyclohexyl nitrite; (c) spectrum of 4-methylcyclohexyl nitrite; (d) background of instrument (spectrum without 4-methylcyclohexyl nitrite).

SCHEME 2 : Mechanism of Formation of Alkyl Nitrites

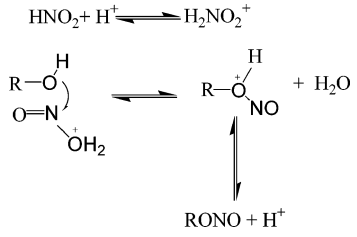

methylcyclohexyl nitrite (>86% pure), *trans*-4-methylcyclohexyl nitrite (>94% pure), and mixture of isomers (>99% pure). The ratio of *trans*- to *cis*-4-methylcyclohexyl nitrite was about 5:2. The liquid nitrite samples were kept at −20 °C when not in use. In the spectroscopic experiments, the vapor of the nitrite precursor was flowed at a partial pressure of 2.0−13 mTorr and was balanced by N_2 (Haun Welding Supplies, 99.999%) up to 50 Torr total pressure. Total pressures of 50 and 90 Torr were used in kinetics experiments.

To estimate the concentration of the mixture of *cis*- and *trans*-4-methylcyclohexoxy produced in the photolysis pulse, we carried out a single measurement of the UV spectrum of 4-methylcyclohexyl nitrite in a 10 cm Pyrex cell with quartz windows. The resultant (approximate) absorption cross section at 351 nm was 1.7×10^{-19} cm^2 molecule^{-1}. Using this value and the photolysis laser fluence of 20 mJ/cm^2, we estimate the initial alkoxy radical concentration to be 2.4×10^{12} molecules/cm^3 at 6.5 mTorr nitrite (or 8×10^{11} molecules/cm^3 at 2.0 mTorr nitrite). As the peak absorption cross-sections of alkyl nitrites appear to be relatively insensitive to molecular structure, and as the cross section varies only by a factor of ∼3 between peaks and troughs in the spectrum,[11,28,39] the initial concentration of the d11-cyclohexoxy radical should be similar to that of 4-methylcyclohexoxy radical. The temperature of the gases inside the cell was varied between 228 and 301 K. The partial pressure of O_2 (Messer, 99.999%) was varied from 0.3 Torr (1.0×10^{16} molecules/cm^3 at 298 K) to 10.0 Torr.

Quantum chemical computations were carried out with the GAUSSIAN98 series of programs[40] using the hybrid exchange functional of Becke and the correlation functional of Lee, Yang, and Parr, a combination denoted B3LYP.[41,42] The B3LYP functional was combined with the 6-31G(d,p) basis set, a combination that typically yields fairly accurate activation barriers to β-scission and H-shift reactions of alkoxy radicals.[43−45] Structures and harmonic vibrational frequencies were obtained for multiple conformers of *cis*- and *trans*-4-methylcyclohexoxy radicals. Transition states were found for the β-scission of the d11-cyclohexoxy radical and the trans isomer of the 4-methylcylohexoxy radical, and for the 1,6 H-shift reaction of the twist-boat conformer of the *cis*-4-methylcylohexoxy radical. Vibrational frequencies were inspected to verify the identity of potential energy minima and transition states.

Results and Discussion

1. LIF Detection of 4-Methylcyclohexoxy and d11-Cyclohexoxy Radicals. Figure 1d shows the instrumental blank obtained by scanning the dye laser from 345 to 376 nm in the absence of nitrite. The background spectrum, depicted in Figure 1c, is obtained by adding d11-cyclohexyl nitrite to the gas flow with the photolysis laser blocked. Strong LIF signals with no clear vibrational structure cover the wavelength region of interest. Although small nitrites are thought to dissociate on an ultrafast time scale (<1 ps) upon photoexcitation,[46,47] some photochemical experiments suggest quantum yields for photodissociation that are less than unity.[48] The overall LIF spectrum arising from both the d11-cyclohexoxy radical and d11-cyclohexyl nitrite obtained when the photolysis laser is unblocked is shown in Figure 1b. Because only ∼1% of the d11-cyclohexoxy nitrite was photolyzed in the chamber, the decrease in spectral intensity due to loss of d11-cyclohexyl nitrite is not detectable against the experimental noise. After subtracting the background spectrum, one obtains Figure 1a: the LIF spectrum arising from d11-cyclohexoxy alone. The spectrum is dominated by the progression labeled A in Figure 1a, which consists of four pairs of peaks, split by ∼76 cm^{-1}, with an interval of ∼640 cm^{-1}. No obvious progression was found involving peaks at an energy lower than 26 698 cm^{-1}. In addition to progression A, there are two other clear progressions that also possess ∼640 cm^{-1} intervals. The apparent origins of these progressions are displaced to higher frequency with respect to each peak in progression A: progression B with four (singlet) peaks, ∼353 cm^{-1} higher; progression C with three (multiplet) peaks, ∼480 cm^{-1} higher.

Several progressions were observed in the spectrum of the normal cyclohexoxy radical, all of which possessed intervals of ∼685 cm^{-1}, and all of which were assigned to the CO stretch.[11,34] It therefore seems very likely that the 640 cm^{-1} progression in the d11-cyclohexoxy radical also arises from the C−O stretch mode. The splitting of 76 cm^{-1} in progression A recalls the ∼60 cm^{-1} splitting in normal cyclohexoxy radical, which Zu et al.[34] suggested was due to the splitting of the $\tilde{X}$ and $\tilde{A}$ states. Note that Zu et al.[34] assigned the $\tilde{B}-\tilde{A}$ and $\tilde{B}-\tilde{X}$ transitions of normal cyclohexoxy to 26 693.1 and 26 754.3 cm^{-1}, respectively. We correspondingly suggest that the strong peaks at 26 698 and 26 774 cm^{-1} are the origin bands of the $\tilde{B}-\tilde{A}$ and $\tilde{B}-\tilde{X}$ transitions, respectively, of the d11-cyclohexoxy radical.

Like cyclohexoxy,[11] d11-cyclohexoxy radical possesses equatorial and axial conformers, as shown below, and the equatorial conformer is expected to dominate:[49]

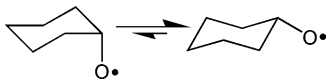

The presence of only a single vibrational interval suggests, as it did for cyclohexoxy, that only one conformer is contributing significantly to the spectrum. Zu et al., carried out a rotational analysis of the spectrum of the cyclohexoxy radical cooled in a supersonic expansion and concluded that the spectra seen in our previous experiments[11] and theirs[34] arose from the equatorial conformer. By analogy to their work, we suggest that the observed spectrum of the d11-cyclohexoxy radical also arises from the equatorial conformer.

The approach described above for d11-cyclohexoxy radicals was used to obtain the LIF spectrum of a mixture of trans and cis isomers of 4-methylcyclohexoxy radicals and distinguish it from that of the nitrite precursor (see Figure 2). The dominant progression marked as A in Figure 2a is found to carry four pairs of peaks starting at 26 836 cm^{-1}, split by ∼71 cm^{-1}, at ∼690 cm^{-1} intervals. No obvious peaks or progressions appear below 26 836 cm^{-1}, which is consistent with previous results for the transition origin of normal cyclohexoxy radicals.[11,34] Three other reproducible progressions with intervals of ∼690 cm^{-1} are designated B, C, and D in Figure 2. The apparent origins of these transitions are shifted to higher frequency with respect to each peak in progression A: progression B with three (singlet) peaks, ∼351 cm^{-1} higher; progression C with three (triplet) peaks, ∼534 cm^{-1} higher; progression D with two (multiplet) peaks, ∼864 cm^{-1}.

Using the same procedure, we obtained the spectrum of the cis and trans isomers of the 4-methylcyclohexoxy radical separately. The *trans*-4-methylcyclohexoxy radical yields the spectrum shown in Figure 3a, which is essentially the same as that obtained from a mixture of *trans*- and *cis*-4-methylcyclohexoxy radicals. The spectrum of pure *cis*-4-methylcyclohexoxy, shown in Figure 3b, was very weak.

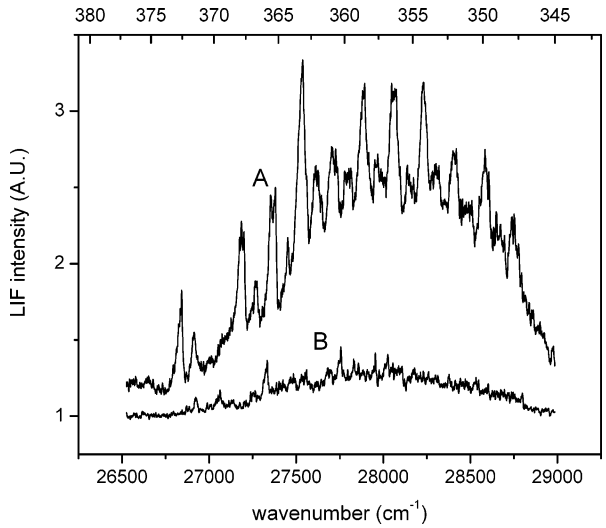

Figure 3. LIF excitation spectra of (A) *trans*-4-methylcycloheoxy radical and (B) *cis*-4-methylcyclohexoxy radical.

trans-4-Methylcyclohexoxy radical has two significant conformers, diequatorial and diaxial:

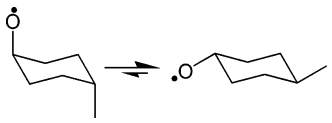

Our B3LYP/6-31G(d,p) calculations indicate that the diequatorial conformer is more stable than the diaxial conformer by 2.7 kcal/mol (see Table 1). This is consistent with estimates of the conformational energies of the analogous closed shell alcohol.[50] If correct, an equilibrium mixture of *trans*-4-methylcyclohexoxy radical at 227 K would contain only 0.2%, and at 298 K, only 1% of the diaxial conformer. The large signal strength (comparable to that obtained for cyclohexoxy or d11-cyclohexoxy) strongly suggests that our signal results from the diequatorial conformer. Although it is possible that nitrite photolysis produces a ratio of conformers that differs significantly from the equilibrium ratio, the spectrum observed from the *trans*-4-methylcyclohexoxy radical does not appear to change shape with time, and the peak intensity decays by less than experimental error in 100 μs (at 298 K in the absence of added O_2). If the spectrum arose from the diaxial conformer, it would be expected to convert to the diequatorial conformer with a half-life of $\sim$10 μs at 298 K.[49] Therefore, the LIF spectrum is assigned to the diequatorial conformer of the *trans*-4-methylcyclohexoxy radical. The similarity of the intervals in normal cyclohexoxy and *trans*-4-methylcyclohexoxy suggest that both spectra arise from conformers with the radical center in the same orientation (equatorial) and support the conformational assignment of normal cyclohexoxy radical made by Zu et al.[34]

2. Reactions of 4-Methylcyclohexoxy and d11-Cyclohexoxy with O_2. The kinetic studies used very large excesses of molecular oxygen to ensure pseudo-first-order conditions. Due to the large cost of the isomerically pure *cis*- or *trans*-4-methylcyclohexanol, which is the starting material for synthesis of the alkoxy radical precursors, the kinetic studies used mixtures of the cis and trans isomers. Because only the trans isomer yields significant fluorescence, the kinetics are attributable to that isomer alone.

Figure 4 shows a typical plot of the natural logarithm of LIF intensity (after correction for background LIF signals) versus delay time for *trans*-4-methylcyclohexoxy in the presence of various concentrations of O_2. Pseudo-first-order reaction rate constants, k^{first}, are calculated from the slopes of each line. We note here that the vibrational structure of the spectrum does not change with delay time, indicating that there is no significant fluorescence from the reaction products. Bimolecular reaction rate constants were obtained from the slopes of linear fits to plots of k^{first} versus the concentration of O_2, examples of which are shown in Figure 5. The high linearity of the data shown in Figures 4 and 5 confirms the applicability of the pseudo-first-order approximation to our experiments.

An Arrhenius plot of the bimolecular rate constants is shown in Figure 6, and the results of each experiment are listed in Table 2. The Arrhenius expression is

$$k_{O2} = (1.0^{+3}_{-0.5}) \times 10^{-13} \exp[(-710^{+320}_{-200})/T] \text{ cm}^3 \text{ molecule}^{-1} \text{ s}^{-1} \quad (228-301 \text{ K})$$

where the cited errors represent two standard deviations of the statistical error, and the weight of each data point was set to the inverse of its uncertainty. On the basis of the Arrhenius fit, the rate constant at 298 K is calculated as $k_{O_2} = 9.2 \times 10^{-15}$ cm^3 molecule^{-1} s^{-1}.

Figure 7 shows the pseudo-first-order loss of d11-cyclohexoxy at several O_2 concentrations. The pseudo-first-order rate constants are plotted versus O_2 concentration in Figure 8. All the bimolecular rate constants are listed in Table 3, and Figure 9 shows the Arrhenius plot. The Arrhenius expression is found to be

$$k_{O_2} = (2.6^{+4}_{-2}) \times 10^{-14} \exp[(-660 \pm 260)/T] \text{ cm}^3 \text{ molecule}^{-1} \text{ s}^{-1} \quad (228-301 \text{ K})$$

The 298 K rate constant derived from the above expression is 2.8×10^{-15} cm^3 molecule^{-1} s^{-1} which, as expected, is much slower than the reaction rate observed for isotopically normal cyclohexoxy radicals (1.8×10^{-14} cm^3 molecule^{-1} s^{-1}).

Arrhenius parameters for other alkoxy radicals reacting with O_2 are listed in Table 4. The Arrhenius preexponential (A) factor reported here for the reaction of *trans*-4-methylcyclohexoxy with O_2 is larger than the A factor found for any other alkoxy radicals except for our previously reported value for the cyclohexoxy radical. The activation energies reported for *trans*-4-methylcyclohexoxy and d11-cyclohexoxy radicals are larger than those of most alkoxy radicals except for methoxy and cyclohexoxy radicals and about 3−4 times higher than the typical value for acyclic secondary alkoxy radicals.[1−3]

Consider the statistical uncertainties reported for the individual rate constant determinations. In the measurements of both *trans*-4-methylcyclohexoxy and d11-cyclohexoxy radicals, standard deviations generally increase with increasing temperature: from 2% at 228 K to 10% at 301 K for 4-methylcyclohexoxy and from 2% at 228 K to 30% at 301 K for d11-cyclohexoxy radical. The trends of uncertainties reflect the enormous impact of competing fates of the alkoxy radicals (other than reaction with O_2) at higher temperatures. Consider the intercepts of our plots of k^{first} vs [O_2], which represent the rates of reactions competing with the O_2 reaction to remove alkoxy radicals. These intercepts are very large at the higher temperatures used here. For *trans*-4-methylcyclohexoxy, the intercept at 301 K (2.1×10^5 s^{-1}) essentially equals the implied pseudo-first-order rate constant (2.2×10^5 s^{-1}) for reaction with O_2 at the highest O_2 concentration used (9×10^{16} molecule/cm^3). Therefore, fluctuations in the rates of these competing reactions contribute significantly to the scatter in the measured bimo-

TABLE 1: Absolute Energies (Hartrees), Zero Point Energies (in Parentheses, kcal/mole), and Relative Energies (kcal/mol, with Respect to the Global Minimum) of Isomers, Conformers, and the Transition State of the 1,6 H-Shift of the 4-Methylcyclohexoxy Radical, at the B3LYP/6-31G(d,p) Level of Theory

	conformation					
	equatorial C−O		axial C−O		twist-boat conformer	
	abs energy	rel energy	abs energy	rel energy	abs energy	rel energy
trans−4-methylcyclohexoxy	−349.75918 (118.0)	0	−349.75531 (118.3)	2.7		
cis−4-methylcyclohexoxy	−349.75597 (118.2)	2.2	−349.75865 (118.1)	0.4	−349.74788 (119.0)	8.1
TS for 1,6 H-shift					−349.73034 (115.6)	15.7
product of 1,6 H-shift					−349.74488 (118.3)	9.3
TS for β-scission	−349.73741 (116.2)	11.8				
Product of β-scission[a]	−349.74500 (114.8)	5.7				

[a] In extended conformation. The identity of product is independent of whether it is formed from *cis*- or *trans*-4-methylcyclohexoxy.

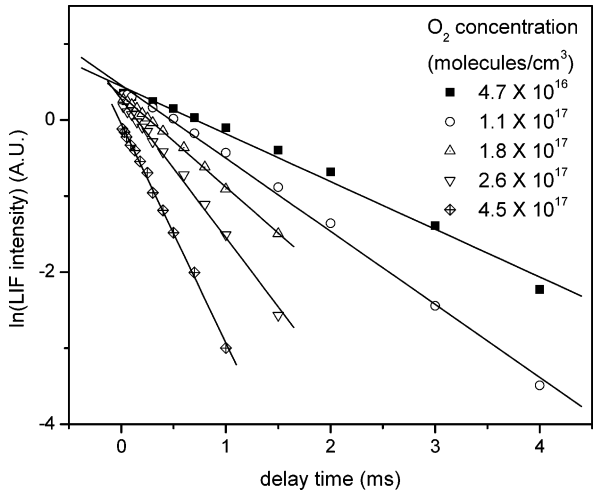

Figure 4. Typical linear decays of ln(LIF intensity) as a function of the delay time for of the *trans*-4-methylcyclohexoxy radical reacting with various concentrations of O_2 at total pressure 50 Torr and 246 K.

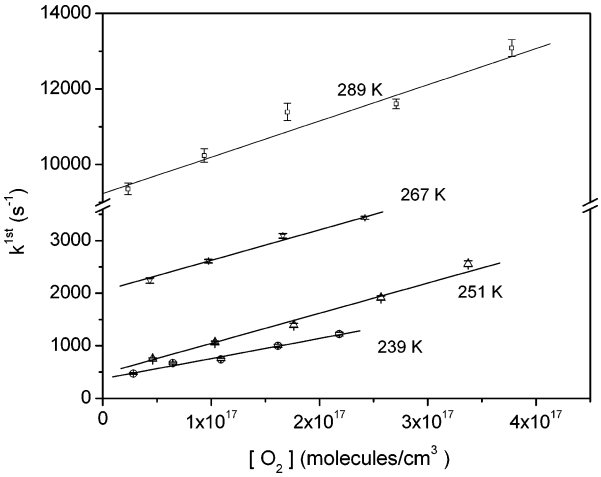

Figure 5. Linear fits of the pseudo-first-order rate constant for loss of *trans*-4-methylcyclohexoxy versus the O_2 concentration at 239, 251, and 267 K.

lecular rate constants at the higher temperatures used here. The uncertainties in the rate constants measured here for the d11-cyclohexoxy radical are higher than those for the *trans*-4-methylcyclohexoxy radical. This is an artifact of the experimental conditions and the much lower rate constant of the O_2 reaction of the d11-cyclohexoxy radical vs the *trans*-4-methylcyclohexoxy radical: we used higher O_2 concentrations for the experiments with the d11-cyclohexoxy radical, and O_2 is an efficient quencher of alkoxy radical fluorescence.[11,28]

In the determination of Arrhenius parameters for both alkoxy radicals, individual rate constants were assigned weights

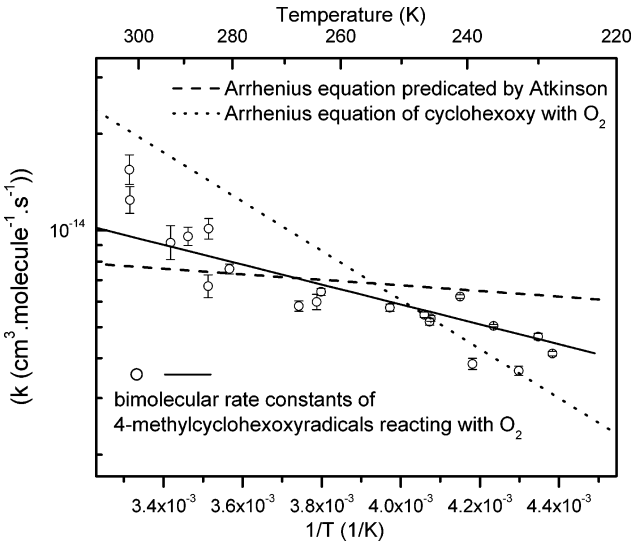

Figure 6. Arrhenius plot showing the temperature dependence of the rate constant for the reaction of *trans*-4-methylcyclohexoxy with O_2.

TABLE 2: Bimolecular Rate Constants of 4-Methylcyclohexoxy Reaction with O_2 at Different Temperatures, Probe (Excitation) Laser Wavelengths, Total Pressure, and RONO Partial Pressures

T (K)	probe laser wavelength (nm)	P (Torr)	RONO partial pressure (mTorr)	k (cm^3 molecule^{-1} s^{-1})
228	354.246	90	6.5	$(4.1 \pm 0.1) \times 10^{-15}$
230	354.246	50	6.5	$(4.7 \pm 0.2) \times 10^{-15}$
233	354.256	90	6.5	$(3.7 \pm 0.2) \times 10^{-15}$
236	354.246	50	2.0	$(5.0 \pm 0.1) \times 10^{-15}$
239	354.246	50	6.5	$(3.8 \pm 0.3) \times 10^{-15}$
241	351.161	50	6.5	$(6.2 \pm 0.2) \times 10^{-15}$
245	354.246	50	6.5	$(5.3 \pm 0.2) \times 10^{-15}$
245	349.910	50	6.5	$(5.2 \pm 0.2) \times 10^{-15}$
246	354.246	50	2.0	$(5.5 \pm 0.2) \times 10^{-15}$
251	354.246	50	6.5	$(5.7 \pm 0.3) \times 10^{-15}$
263	354.246	50	2.0	$(6.4 \pm 0.3) \times 10^{-15}$
264	351.161	90	6.5	$(6.0 \pm 0.7) \times 10^{-15}$
267	354.246	50	6.5	$(5.8 \pm 0.5) \times 10^{-15}$
280	349.910	50	6.5	$(7.6 \pm 0.5) \times 10^{-15}$
285	354.246	90	6.5	$(1.0 \pm 0.1) \times 10^{-14}$
285	354.246	50	6.5	$(6.8 \pm 1.0) \times 10^{-15}$
289	349.910	50	6.5	$(9.6 \pm 1.2) \times 10^{-15}$
293	354.246	50	6.5	$(9.2 \pm 2.2) \times 10^{-15}$
301	354.261	50	6.5	$(1.2 \pm 0.2) \times 10^{-14}$
301	354.261	50	6.5	$(1.5 \pm 0.3) \times 10^{-14}$

inversely proportional to their relative uncertainties. This is why the highly uncertain data points near room temperature do not bracket the Arrhenius fit in Figure 6 or, much more noticeably, in Figure 9. The deviation of the room temperature data from the Arrhenius fit is discussed extensively in section 3 of the Results and Discussion.

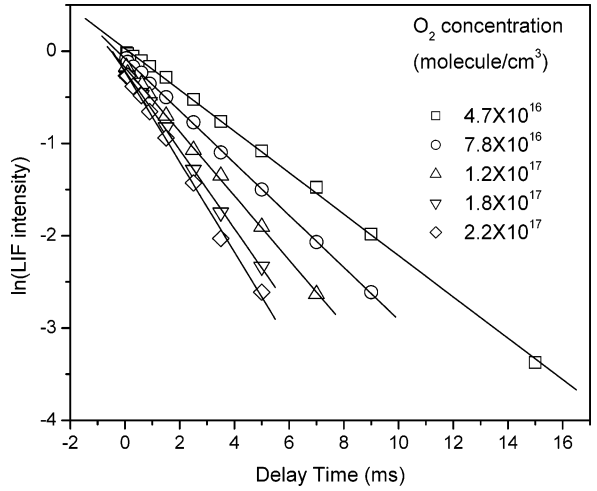

Figure 7. Typical linear decays of ln(LIF intensity) as a function of the delay time for d11-cyclohexoxy reacting with various concentrations of O_2 at total pressure 50 Torr and 231 K.

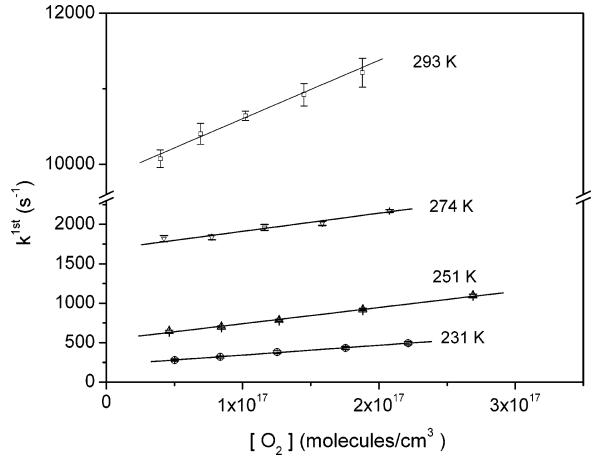

Figure 8. Linear fits of the pseudo-first-order rate constant for loss of d11-cyclohexoxy versus the O_2 concentration at 231, 251, and 274 K.

TABLE 3: Bimolecular Rate Constants of d11-Cyclohexoxy Reaction with O_2 at Different Temperatures, Probe (Excitation) Laser Wavelengths, Total Pressure, and RONO Partial Pressures

T (K)	probe laser wavelength (nm)	P (Torr)	RONO partial pressure (mTorr)	k (cm^3 molecule^{-1} s^{-1})
228	347.446	50	6.5	$(1.5 \pm 0.1) \times 10^{-15}$
231	347.446	50	6.5	$(1.2 \pm 0.2) \times 10^{-15}$
239	347.446	50	6.5	$(1.9 \pm 0.1) \times 10^{-15}$
239	365.732	50	2.6	$(1.4 \pm 0.1) \times 10^{-15}$
243	347.446	50	6.5	$(1.8 \pm 0.1) \times 10^{-15}$
243	347.446	50	6.5	$(1.2 \pm 0.3) \times 10^{-15}$
247	365.732	90	6.5	$(1.6 \pm 0.1) \times 10^{-15}$
247	352.802	50	6.5	$(1.7 \pm 0.1) \times 10^{-15}$
251	347.446	50	6.5	$(2.0 \pm 0.2) \times 10^{-15}$
255	347.446	50	2.6	$(1.7 \pm 0.1) \times 10^{-15}$
257	347.447	50	6.5	$(2.0 \pm 0.1) \times 10^{-15}$
267	347.447	50	6.5	$(2.4 \pm 0.4) \times 10^{-15}$
274	365.732	50	6.5	$(2.5 \pm 0.5) \times 10^{-15}$
275	352.802	90	6.5	$(2.3 \pm 0.4) \times 10^{-15}$
275	365.732	50	13	$(2.5 \pm 0.6) \times 10^{-15}$
284	347.447	50	6.5	$(3.5 \pm 1.8) \times 10^{-15}$
293	347.446	50	13	$(7.7 \pm 2.4) \times 10^{-15}$
301	347.446	50	6.5	$(2.4 \pm 1.4) \times 10^{-14}$

The large differences between the Arrhenius parameters for *trans*-4-methylcyclohexoxy and normal cyclohexoxy is baffling and motivates us to consider some potential confounding factors.

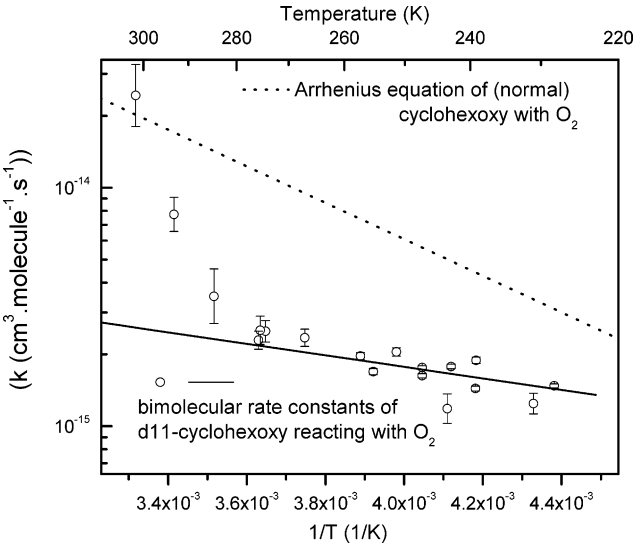

Figure 9. Arrhenius plot showing the temperature dependence of the rate constant for the reaction of d11-cyclohexoxy with O_2.

Reaction of alkoxy radicals with other radicals, such as O atom, OH, or HO_2 might undermine accurate measurement of k^{first} and k_{O_2}. To determine if this sort of secondary radical chemistry is a problem, we reduced the nitrite (radical precursor) concentration by a factor of 3 and repeated the rate constant determinations at three temperatures (see Tables 2 and 3). However, the three rate constants obtained using one-third the initial radical concentration are indistinguishable from those obtained at the higher radical concentrations used in most of the experiments. This makes it extremely unlikely that secondary radical chemistry is significantly affecting our determination of k_{O_2}.

A second test of the potential for secondary radical chemistry was carried out by modeling the side reactions at 228 and 301 K. We tried to make this model a stringent test of the potential for secondary radical chemistry by (1) modeling d11-cyclohexoxy (which has the slowest rate of reaction with O_2 of the three radicals of interest), (2) using the lowest experimental O_2 concentration (5×10^{16} molecules/cm^3), and (3) maximizing the assumed value of the rate constants for d11-cyclohexoxy self-reaction and the reaction d11-cyclohexoxy + DO_2 (1×10^{-10} cm^3 molecule^{-1} s^{-1}). Under these conditions, the biggest loss process for the d11-cyclohexoxy radical was reaction with d11-cyclohexyl nitrite. For this reaction, we assigned a rate constant of 4×10^{-12} cm^3 molecule^{-1} s^{-1} (which corresponds to the reported rate constant for the RO + RONO reactions of other alkoxy radicals, excluding R=CH_3).[25,29,30] The dominance of the (pseudo-first order) RO$^{\bullet}$ + RONO reaction in the model confirms that secondary radical chemistry should not interfere with our analysis.

As noted previously and depicted in Figures 1 and 2, the kinetic experiments used three different excitation (probe) wavelengths for each radical. Because results from all three wavelengths are consistent within the scatter of the data, it is unreasonable to suggest that other fluorescing species are significantly interfering with our determinations. One must consider, however, the inversion reaction of these radicals. The approximate lifetime of the inversion reaction for monosubstituted cyclohexanes in solution is $\sim$5 μs at room temperature and $\sim$1 ms at 228 K.[49,50] The time scale for kinetic measurements is 10 μs to 15 ms in our experiments, so the inversion may well be occurring in our experiments. In the case of *trans*-4-methylcyclohexoxy, equilibrium favors the diequatorial con-

SCHEME 3 : Reactions Controlling the Fate of the Cyclohexoxy Radical in Our Experiments

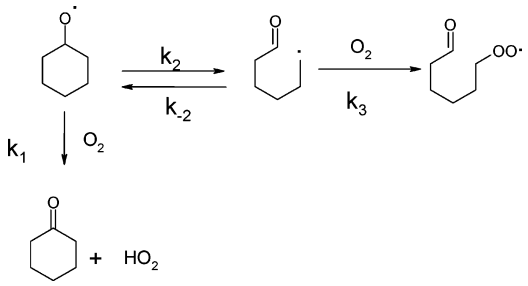

former so strongly that conformational interchange cannot significantly affect the kinetics. However, if conformational interchange was affecting the measured concentration of d11-cyclohexoxy radical, we would expect to see nonlinearities in some of our plots of ln(intensity) versus time shown in Figure 7. Because we observe neither of these behaviors, we conclude that conformational interchange, though possibly occurring to a significant extent in some of our experiments, is not greatly affecting our kinetic results.

The above discussion suggests no obvious sources of error that would explain the activation energies for the O_2 reactions of *trans*-4-methylcyclohexoxy and d11-cyclohexoxy radicals being 3−4 times higher than the recommended values, nor for the difference between the Arrhenius parameters of *trans*-4-methylcyclohexoxy versus the normal cyclohexoxy radical.

3. Modeling the Influence of Scission on Measure Rate Constants. If we were working with *acyclic* alkoxy radicals, the scission reactions would not affect the determination of bimolecular rate constants. However, consider the effect of $[O_2]$ on the concentration of cyclic alkoxy radicals, as depicted for cyclohexoxy radical in Scheme 3.

At the low $[O_2]$ used in our experiments, the 6-oxohexyl radicals formed in the scission reaction might transform back to alkoxy radicals via reaction (−2) at rates competitive with the removal of the 6-oxohexyl radical via reaction with O_2 (reaction 3). Due to the strong temperature dependence of reaction 2, the effect of $[O_2]$ on the competition between reactions (3) and (−2) will be much more apparent at high temperature than at low temperature. Because our Arrhenius fits of alkoxy + O_2 rate constants are weighted heavily by the low temperature data, the Arrhenius parameters may be fairly accurate representations of the bimolecular rate constants despite this problem. Recall that the measured alkoxy + O_2 rate constants at the upper end of the temperature range studied are higher than the Arrhenius fit to the rate constants (see Figures 6 and 9). Note that the fitted high-temperature rate constants for the alkoxy + O_2 reactions increase in the order d11-cyclohexoxy < 4-methylcyclohexoxy < normal cyclohexoxy, so the influence of the reverse scission reaction (−2) is likely to be most important for d11-cyclohexoxy and least important for normal cyclohexoxy. This is qualitatively consistent with the extent of the temperature range over which the measured alkoxy + O_2 rate constants deviate significantly from the Arrhenius fits: $T \geq 284$ K for d11-cyclohexoxy, $T = 301$ K for *trans*-4-methylcyclohexoxy, and not at all for normal cyclohexoxy radical.[11]

A reasonable kinetic model can be constructed to determine, semiquantitatively, the feasibility of this explanation for the deviation of the high-temperature data from the Arrhenius fits. The idea is to analyze the modeled loss rate of alkoxy radicals, in the same manner as experiment, to determine the *apparent*

TABLE 4: Arrhenius Parameters for the Reactions of Various Alkoxy Radicals with O_2

radical	$10^{15}A$ (cm^3 molecule^{-1} s^{-1})	E_a/R	T range (K)	ref
CH_3O	55	1000	298−450	17
C_2H_5O	71	550	295−411	19
	24	325	295−354	24
1-C_3H_7O	14	110	223−303	21
	25	240	289−381	24
2-C_3H_7O	10	220	218−313	21
	15	190	298−383	18
	16	265	288−364	24
2-C_4H_9O	23	170	223−305	60
3-pentoxy	4.1	−310	220−285	28
cyclohexoxy	5850	1720	225−302	11
Secondary alkoxy	15	200	<600	1
trans-4-methylcyclohexoxy[a]	100	710	228−301	this
	(140)	(810)	(228−292)	work
d11-cyclohexoxy[a]	26	660	228−301	this
	(37)	(760)	(228−267)	work

[a] Values in parentheses arise out of the elimination of higher-temperature data points from our analysis, as justified in see section 3 of the Results and Discussion.

TABLE 5: Arrhenius Parameters of Reverse Scission Reaction (−2 in Scheme 3) at 50 Torr Calculated Using the B3LYP/6-31G(d,p) (Asterisked) Activation Barrier and Barriers Incremented in Steps of 2 kcal/mol

trans-4-methylcyclohexoxy	barrier (kcal/mol)	6.2*	8.2	10.2
	$10^{-10}A$ (s^{-1})	4.5	5.3	5.5
	E_a (kcal/mol)	5.4	7.5	9.5
d11-cyclohexoxy	barrier (kcal/mol)	6.9*	8.9	10.9
	$10^{-10}A$ (s^{-1})	1.6	1.7	1.8
	E_a (kJ/mol)	6.1	8.1	10.1

bimolecular rate constants for the alkoxy + O_2 reactions. If Scheme 3 captures the chemistry important in our experiment, then the modeled and experimental rate constants should agree with each other and disagree with the Arrhenius parameters near room temperature. Using the numbering system of Scheme 3, and generalizing it to all three cyclic alkoxy radicals considered here, we take k_1 from the Arrhenius fits reported here and in ref 11, and 8×10^{-12} cm^3 molecule^{-1} s^{-1} as a reasonable value for k_3.[51] The activation barrier to the scission reactions (2) were calculated for d11-cyclohexoxy and 4-methylcyclohexoxy at B3LYP/6-31G(d,p). Absolute and relative energies are reported in Table 1, and the Arrhenius parameters were calculated at 50 Torr N_2 using the UNIMOL program[52] in the same manner as we previously calculated the rate for the normal cyclohexoxy radical.[11]

$$k_{\text{scission,4-mecyc}} = 1.8 \times 10^{13} \exp(-12.2\ (\text{kcal/mol})/RT)\ \text{s}^{-1}$$

$$k_{\text{scission,d11-cyc}} = 2.4 \times 10^{13} \exp(-12.4\ (\text{kcal/mol})/RT)\ \text{s}^{-1}$$

Although B3LYP/6-31G(d,p) has generally performed well in calculating barriers to the β-scission of alkoxy radicals, as noted previously, it often does poorly for the energy of reaction,[53−55] which creates a large uncertainty in k_{-2}. Therefore, k_{-2} was calculated three times, allowing the value of the barrier height to be incremented in steps of 2.0 kcal/mol and recalculating the 50 Torr rate constant using UNIMOL. Table 5 reports the resulting Arrhenius fits to the 50 Torr rate constants.

The kinetic model was run using the program KINTECUS[56] at a range of $[O_2]$ spanning the range used in the present experiments. At each $[O_2]$, a k^{first} for loss of alkoxy was determined from the slope of a plot of the natural logarithm of the computed concentration versus time, and these values of k^{first} were plotted vs $[O_2]$ (analogous to Figures 5 and 8) to

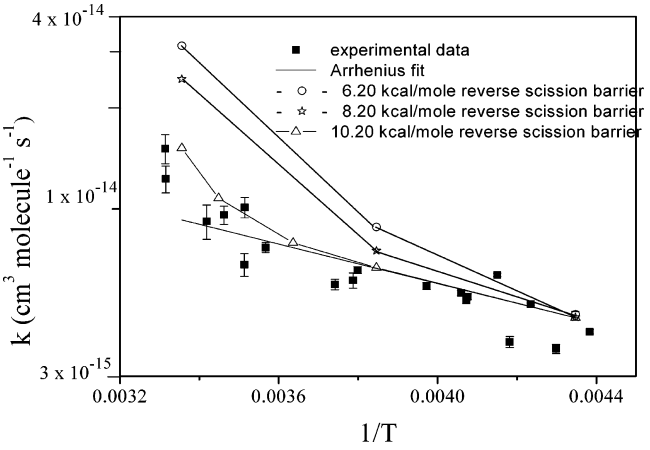

Figure 10. Comparison of experimental and modeled (based in Scheme 3) apparent rate constants for *trans*-4-methylcyclohexoxy reacting with O_2.

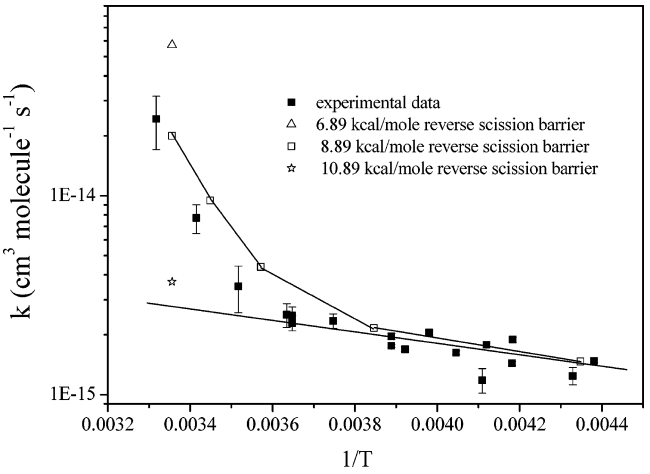

Figure 11. Comparison of experimental and modeled (based in Scheme 3) apparent rate constants for d11-cyclohexoxy reacting with O_2.

extract apparent bimolecular rate constants for the alkoxy + O_2 reaction. This process was repeated at several temperatures spanning the range used in these experiments. Under the experimental conditions, plots of the natural logarithm of the computed concentration versus time were linear; these plots would show strong nonlinearities if extended to lower [O_2], as would plots of k^{first} for loss of alkoxy vs [O_2].

Figures 10 and 11 show the results for the *trans*-4-methylcyclohexoxy and d11-cyclohexoxy radicals, respectively. The experimental data are best fit if the activation barrier to reaction (−2) is 4.0 and 2.0 kcal/mol higher than the B3LYP/6-31G(d,p) values for *trans*-4-methylcyclohexoxy and d11-cyclohexoxy, respectively. An error this large in the B3LYP reaction energy is quite reasonable.[43,45,54,55] Also, it should be noted we only considered a single (extended) conformer of the product of β-scission. Not only is it the case that this conformer might not have been the lowest-energy conformer, but also the impact of multiple conformations[57] on k_{-2} was not taken into account; both of these factors would tend to make the true rate constant, k_{-2}, lower than suggested by B3LYP/6-31G(d,p). For the normal cyclohexoxy radical, the model indicates an insignificant effect of reaction (−2) on the alkoxy radical loss rate, which is consistent with the effect of the magnitude of k_1 on the importance of Scheme 3 to the rate of loss of the alkoxy radical. Therefore, we suggest this mechanism as a feasible explanation for the deviation of the high-temperature data from the Arrhenius fit. We suggest the following revised Arrhenius fits over more limited temperature ranges as more reliable representations of the actual rate of the elementary alkoxy + O_2 reactions:

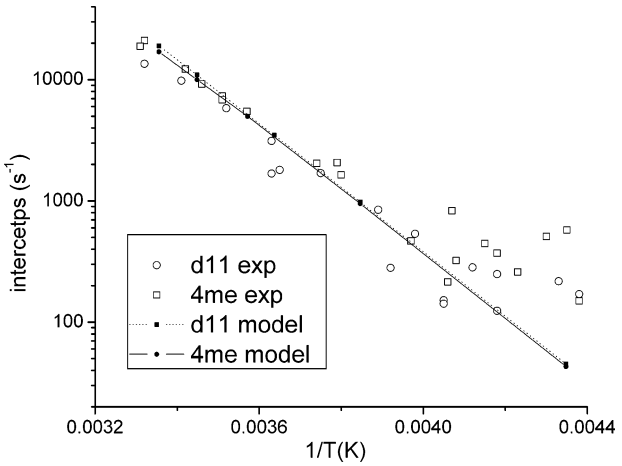

Figure 12. Arrhenius plot showing the temperature dependence of the intercepts of our plots of pseudo-first-order rate constant versus the O_2 concentration. Both modeled and experimental results are shown, along with the fit to the model results.

trans-4-methylcyclohexoxy (228−292 K)

$$k_{O_2} = (1.4^{+8}_{-1}) \times 10^{-13} \exp[(-810 \pm 400)/T] \text{ cm}^3 \text{ molecule}^{-1} \text{ s}^{-1}$$

d11-cyclohexoxy (228−267 K)

$$k_{O_2} = (3.7^{+4}_{-1}) \times 10^{-14} \exp[(-760 \pm 400)/T] \text{ cm}^3 \text{ molecule}^{-1} \text{ s}^{-1}$$

These cyclic alkoxy + O_2 reactions would be effectively irreversible at 1 atm of air at 298 K; the low (1−10 Torr) concentrations of O_2 used in these experiments adds this complexity to the kinetics at the higher temperatures studied here. Note, also, that β-scission is effectively irreversible for *acyclic* alkoxy radicals even at the lowest [O_2] used in these experiments.

Let us consider the intercepts of our of plots of k^{first} versus O_2 (Figures 5 and 8). Figure 12 depicts the modeled and experimental intercepts, along with the fit to the modeled intercepts. Note that modeled and experimental intercepts agree well at temperatures above 250 K. This supports the accuracy of the model used to evaluate the effect of Scheme 3 on the observed rate of these alkoxy + O_2 reactions.

Finally, let us consider the 1,6 H-shift of *cis*-4-methylcyclohexoxy, relative energies of which are listed in Table 1. This reaction would appear to be slow, because the transition state lies 7.6 kcal/mol above the twist-boat conformer, which, in turn, is 7.7 kcal/mol higher than the most stable conformer of *cis*-4-methylcyclohexoxy. Therefore, the activation energy of the 1,6 H-shift is effectively 15.3 kcal/mol. The *A* factor for the 1,6 H-shift in alkoxy radicals has been computed to be about 70 times lower[58] than the *A* factor for the 1,5 H-shift ($\sim 2 \times 10^{12}$ s^{-1} at 1 atm).[59] Therefore, the 1,6 H-shift should be

$$k_{iso,CH_3} = 3 \times 10^{10} \exp[-15.3 \text{ kcal/mol}/RT] \text{ s}^{-1} = 0.2 \text{ s}^{-1} (298 \text{ K})$$

This reaction will be unimportant to the fate of *cis*-4-methylcyclohexoxy under atmospheric conditions.

Conclusion

We have reported the first observation of the LIF excitation spectra of *trans*-4-methylcyclohexoxy and d11-cyclohexoxy radicals. Both spectra are consistent with a single conformer, and thermodynamic analysis of the conformers of *trans*-4-methylcyclohexoxy indicates that the radical center must occupy the equatorial position. The rate constants for the O_2 reaction of both alkoxy radicals have been measured by directly monitoring the disappearance of the radicals with LIF. The affect of O_2 concentration on the competition between the reversal of the β-scission reaction and the removal of the product of β-scission has been analyzed. This competition may explain the tendency of our higher-temperature data to deviate upward from the Arrhenius fits, which are largely controlled by the lower-temperature data.

Acknowledgment. We thank the National Science Foundation for support under Grants ATM-0087057 and CHE-0243959. We thank B. S. Hudson for the loan of the hardware for data acquisition, J. P. Hassett for support in GC/MS work, and T. A. Miller for helpful discussions about spectra of cyclohexoxy radicals.

Supporting Information Available: Cartesian coordinates of radicals and transition states at B3LYP/6-31G(d,p) are available free of charge via the Internet at http://pubs.acs.org.

References and Notes

(1) Atkinson, R. *J. Phys. Chem Ref. Data Monograph No. 2*, **1994**.
(2) Atkinson, R. *Int. J. Chem. Kinet.* **1997**, *29*, 99.
(3) Orlando, J. J.; Tyndall, G. S.; Wallington, T. J. W. *Chem. Rev.* **2003**, *103*, 4657.
(4) Jenkin, M. E.; Hayman, G. D. *Atmos. Environ.* **1999**, *33*, 1275.
(5) Schauer, J.; Kleeman, M.; Cass, G.; Simoneit, B. R. T. *Environ. Sci. Technol*. **2002**, *36*, 1169.
(6) Platz, J.; Sehested, J.; Nielsen, O. J. *J. Phys. Chem. A* **1999**, *103*, 2688.
(7) Orlando, J. J.; Iraci, L. T.; Tyndall, G. S. *J. Phys. Chem. A* **2000**, *104*, 5072.
(8) Aschmann, S. M.; Chew, A. A.; Arey, J.; Atkinson, R. *J. Phys. Chem. A* **1997**, *101*, 8042.
(9) Takagi, H.; Washida, N.; Bandow, H.; Akimoto, H.; Okuda M., *J. Phys. Chem.* **1981**, *85*, 2701.
(10) Kavouras, I. G.; Mihalopoulus, N.; Stephanou, E. *Nature* **1998**, *395*, 683.
(11) Zhang, L.; Kitney, K. A.; Ferenac, M. A.; Deng, W.; Dibble, T. S. *J. Phys. Chem. A* **2004**, *108*, 447.
(12) Jungkamp, T. P. W.; Seinfeld, J. H. *Chem. Phys. Lett.* **1996**, *263*, 371.
(13) Bofill, M. J.; Olivella, S.; Sole, A.; Anglada, J. M. *J. Am. Chem. Soc.* **1999**, *121*, 1337**.**
(14) Setokuchi, O.; Sato, M. *J. Phys. Chem. A* **2002**, *106*, 8124.
(15) Sanders, N.; Butler, J. E.; Pasternack. L. R.; McDonald, J. R. *Chem. Phys.* **1980**, *48*, 203.
(16) Gutman, D.; Sanders, N.; Butler, J. E. *J. Phys. Chem.* **1982**, *86*, 66.
(17) Lorenz, K.; Rhasa, D.; Zellner, R.; Fritz, B. *Ber. Bunsen-Ges. Phys. Chem.* **1985**, *89*, 341.
(18) Balla, R.; Nelson, H. H. and McDonald, J. R. *Chem. Phys.* **1985**, *99*, 323.
(19) Hartmann, D.; Karthauser, J.; Sawerysyn, J. P.; Zellner, R. *Ber. Bunsen-Ges. Phys. Chem.* **1990**, *94*, 639.
(20) Frost, M. J.; Smith, I. W. M. *J. Chem. Soc., Faraday Trans.* **1990**, *86*, 1757.
(21) Mund, C.; Fockenberg, C.; Zellner, R. *Ber. Bunsen-Ges. Phys. Chem.* **1998**, *102*, 709.
(22) Devolder, P.; Fittschen, Ch.; Frenzel, A.; Hippler, H.; Poskrebyshev, G.; Striebel, F.; Viskolcz, B. *Phys. Chem. Chem. Phys.* **1999**, *1*, 675.
(23) Caralp, F.; Devolder, P.; Fittschen, C.; Gomez, N.; Hippler, H.; Mereau, R.; Rayez, M. T.; Striebel, F.; Viskolcz, B. *Phys. Chem. Chem. Phys.* **1999**, *1*, 2935.
(24) Fittschen, C.; Frenzel, A.; Imrik K.; Devolder, P. *Int. J. Chem. Kinet.* **1999**, *31*, 860.
(25) Blitz, M.; Pilling, M. J.; Robertson, S. H.; Seakins, P. W. *Phys. Chem. Chem. Phys.* **1999**, *1*, 73.
(26) Wang, C.; Shemesh, L. G.; Deng, W.; Lilien, M. D.; Dibble, T. S. *J. Phys. Chem. A* **1999**, *103*, 8207.
(27) Wang, C.; Deng, W.; Shemesh, L. G.; Lilien, M. D.; Katz, D. R.; Dibble, T. S. *J. Phys. Chem. A* **2000**, *104*, 10368.
(28) Deng, W.; Davis, A. J.; Zhang, L.; Katz, D. R.; Dibble, T. S. *J. Phys. Chem. A* **2001**, *105*, 8985.
(29) Fittschen, C.; Hippler, H.; Viskolcz, B. *Phys. Chem. Chem. Phys.* **2000**, *2*, 1677.
(30) Lotz, C.; Zellner, R. *Phys. Chem. Chem. Phys.* **2000**, *2*, 2353.
(31) Carter, C. C.; Gopalakrishnan, S.; Atwell, J. R.; Miller, T. A. *J. Phys. Chem. A* **2001**, *105*, 2925.
(32) Gopalakrishnan, S.; Carter, C. C.; Zu, L.; Stakhursky, V.; Tarczay, G.; Miller, T. A. *J. Chem. Phys.* **2003**, *118*, 4954.
(33) Gopalakrishnan, S.; Zu, L.; Miller, T. A. *J. Phys. Chem A.* **2003**, *107*, 5189.
(34) Zu, L.; Liu, J.; Tarczay, G.; Dupre, P.; Miller, T. A. *J. Chem. Phys.* **2004**, *120*, 10579.
(35) Zu, L.; Liu, J.; Gopalakrishnan, S.; Miller, T. A. *Can. J. Chem.* **2004**, *82* 854−866.
(36) Blatt, A. H. *Organic Syntheses*; Wiley: New York, 1966; pp 108−109.
(37) Williams, D. L. H. *Nitrosation*; Cambridge University Press: New York, 1988.
(38) Typical alkylnitrite IR and NMR spectra may be found in the Sadtler Index, Bio-Rad Laboratories Inc., 1973.
(39) Calvert, J. G.; Pitts, J. N., Jr. *Photochemistry*; Wiley: New York, 1966.
(40) Frisch, M. J.; Trucks, G. W.; Schlegel, H. B.; Gill, P. M. W.; Johnson, B. G.; Robb, M. A.; Cheeseman, J. R.; Keith, T.; Petersson, G. A.; Montgomery, J. A.; Raghavachari, K.; Al-Laham, M. A.; Zakrzewski, V. G.; Ortiz, J. V.; Foresman, J. B.; Cioslowski, J.; Stefanov, B. B.; Nanayakkara, A.; Challacombe, M.; Peng, C. Y.; Ayala, P. Y.; Chen, W.; Wong, M.; Andres, J. L.; Replogle, E. S.; Gomperts, R.; Martin, R. L.; Fox, D. J.; Binkley, J. S.; Defrees, D. J.; Baker, J.; Stewart, J. P.; Head-Gordon, M.; Gonzalez, C.; Pople, J. A. *Gaussian98*, Revision D.3; Gaussian, Inc.: Pittsburgh, PA, 1995.
(41) Lee, C.; Yang, W.; Parr, R. G. *Phys. Rev. B* **1988**, *37*, 785.
(42) Becke, A. D. *J. Chem. Phys.* **1993**, *98*, 5648.
(43) Peeters, J.; Fantechi, G.; Vereecken, L. *J. Atmos. Chem.* **2004**, *48*, 59.
(44) Orlando, J. J.; Tyndall, G. S.; Bilde, M.; Ferronato, C.; Wallington, T. J.; Vereecken, L.; Peeters, J. *J. Phys. Chem. A* **1998**, *102*, 8116.
(45) Dibble, T. S. *J. Phys. Chem. A* **1999**, *103*, 8559.
(46) Reisler, H.; Noble, M.; Wittig, C. In *Molecular Photodissociation Dynamics*; Ashfold, M. N. R., Baggott, J. E., Eds.; Royal Society: London, 1987.
(47) Untch, A.; Schinke, R.; Cotting, R.; Huber, J. R.. *J. Chem. Phys.* **1993**, *99*, 9553−66.
(48) Heicklen, J. *Adv. Photochem.* **1988**, *14*, 177.
(49) Eliel, E. L.; Wilen, S. H. *Stereochemistry of Organic Compounds*; Wiley: New York, 1994.
(50) Carey F. A. and Sundberg, R. J. *Part A: Structure and Mechanisms*; Advanced Organic Chemistry, 2nd ed.; Plenum Press, New York, 1984.
(51) Atkinson, R.; Baulch, D. L.; Cox, R. A.; Hampson, R. F.; Kerr, J. A.; Rossi, M. J.; Troe, J. *J. Phys. Chem. Ref. Data* **1997**, 521.
(52) Gilbert, R. G.; Smith, S. C.; Jordan, M. J. T. UNIMOL program suite (calculation of falloff curves for unimolecular and recombination reactions), 1993. Available from the authors: School of Chemistry, Sydney University, NSW 2006, Australia or by e-mail to: gilbert_r@summer.chem.su.oz.au.
(53) Jungkamp, T. P. W.; Smith, J. N.; Seinfeld, J. H. *J. Phys. Chem. A* **1997**, *101*, 4392.
(54) Somnitz, H.; Zellner, R. *Phys. Chem. Chem. Phys*. **2000**, *2*, 1899.
(55) Ferenac, M. A.; Davis, A. J.; Holloway, A. S.; Dibble, T. S. *J. Phys. Chem. A* **2003**, *107*, 63.
(56) Ianni, J. C. *Kintecus V3.50*, 1995−2005.
(57) Vereecken, L.; Peeters, J. *J. Chem. Phys*. **2003**, *119*, 5159.
(58) Dorigo, A. E.; Houk, K. N. *J. Org. Chem.* **1988**, *53* 1650.
(59) Somnitz, H.; Zellner, R. *Phys. Chem. Chem. Phys.* **2000**, *2*, 1907.
(60) Zellner, R.; Lotz, Ch. *Phys. Chem. Chem. Phys.* **2001**, *3*, 2607.